REPORT DOCUMENTATION PAGE

Form Approved
OMB No. 0704-0188

1. AGENCY USE ONLY (Leave blank)	2. REPORT DATE	3. REPORT TYPE AND DATES COVERED
	May 07th, 1997	Final Report 5-1-97-12-31-97

4. TITLE AND SUBTITLE

Theoretical Analysis of Powder Size Distribution

5. FUNDING NUMBERS

Grant no. F49620-97-1-0301

6. AUTHOR(S)

Enrique J. Lavernia

7. PERFORMING ORGANIZATION NAME(S) AND ADDRESS(ES)

Department of Chemical, Biochemical Engineering and
Materials Science, University of California, Irvine, CA, 92697-2575

8. PERFORMING ORGANIZATION REPORT NUMBER

9. SPONSORING / MONITORING AGENCY NAME(S) AND ADDRESS(ES)

AFOSR/NA
110 DUNCAN AVENUE SUITE B115
BOLLING AFB DC. 20332-8080

10. SPONSORING / MONITORING AGENCY REPORT NUMBER

11. SUPPLEMENTARY NOTES

12a. DISTRIBUTION / AVAILABILITY STATEMENT

Approved for public release; distribution unlimited.

12b. DISTRIBUTION

13. ABSTRACT *(Maximum 200 words)*

The procedure conventionally employed to interpret the experimental sieving data was examined. It was demonstrated that the conventional procedure is inherently flawed in several aspects. Along with several implicit, hard-to-be-justified assumptions associated with it, the conventional graphical representation procedure also failed to address the reliability of the results. To resolve these problems, a new procedure was formulated. Application of the formulated procedure to several sets of sample sieving data reveals that it is capable of extracting the total weight of powders from experimental data, of determining the nature of the size distribution, of establishing the characteristic parameters, and simultaneously, of determining the reliability of the results. It is anticipated that the accomplishment achieved in the present study will generate significant impact on the understanding and the development of powder related processing technologies, including conventional powder metallurgy, conventional spray atomization, and novel spray processing techniques such as spray atomization and deposition, plasma spray forming, and thermal spray forming.

14. SUBJECT TERMS	15. NUMBER OF PAGES
powder size distribution; sieving data; interpretation procedure	32
	16. PRICE CODE

17. SECURITY CLASSIFICATION OF REPORT	18. SECURITY CLASSIFICATION OF THIS PAGE	19. SECURITY CLASSIFICATION OF ABSTRACT	20. LIMITATION OF ABSTRACT
UNCLASSIFIED	UNCLASSIFIED	UNCLASSIFIED	UL

FINAL REPORT

THEORETICAL ANALYSIS OF POWDER SIZE DISTRIBUTION

Grant Number: F49620-97-1-0301
Cumulatrive Funds Awarded: $16,078.
Period of Performance: 05/01/97 to 12/31/97

Submitted to:
Dr. C.I. CHANG
Director of Aerospace and Materials Sciences
Air Force Office of Scientific Research
AFOSR/NA
110 DUNCAN AVENUE SUITE B115
BOLLING AFB DC. 20332-8080

Submitted by:
Enrique J. Lavernia, Professor and Chair
Department of Chemical, Biochemical
Engineering and Materials Science
University of California, Irvine,
California, 92697-2575
May 07th, 1997

PREFACE

This final report covers the work accomplished during the period from May 1, 1997 to December 31, 1997 under the Air Force Office of Scientific Research (AFOSR) contract F49620-97-1-0301.

Knowledge of the powder size distribution is essential to characterize a collection of powders (either experimental samples or commercial products), and informative to optimize the processing parameters in many powder related manufacturing techniques, both conventional and novel. Sieving analysis is a well-established technique to characterize the powder size distribution. Nevertheless, accurate information on the powder size distribution necessitates an appropriate procedure to interpret the experimentally obtained sieving data. To that effect, the conventional procedure was scrutinized in the present study. It was demonstrated that the conventional procedure is inherently flawed in several aspects. Along with several implicit, hard-to-be-justified assumptions associated with it, the conventional graphical representation procedure also failed to address the reliability of the results. To resolve these problems, a new procedure was formulated. Application of the formulated procedure to several sets of sample sieving data reveals that it is capable of extracting the total weight of powders from experimental data, of determining the nature of the size distribution, of establishing the characteristic parameters, and simultaneously, of determining the reliability of the results. It is anticipated that the accomplishment achieved in the present study will generate significant impact on the understanding and the development of powder related processing technologies, including conventional powder metallurgy, conventional spray atomization, and novel spray processing techniques such as spray atomization and deposition, plasma spray forming, and thermal spray forming.

TABLE OF CONTENTS

LIST OF PUBLICATIONS

resulting from AFOSR Grant no. F49620-97-1-0301

1. "Analysis of Sieving Data in Reference to Powder Size Distribution", Bing Li and E.J. Lavernia, *Acta Materialia*, **vol.** 46, **no.** 2, pp. 617-629 (1998).

CHAPTER 1. INTRODUCTION

Experimental data on powder size distribution analysis may be tabulated or graphically presented. It is widely acknowledged that the most accurate representation of powder size distribution data is in tabular form, in which experimental data are listed as shown in Table 1. It is also realized, however, that graphical representation of experimental data has many advantages over tabulated results, as discussed in detail in references [1] and [2]. Moreover, unless it is graphically presented, the tabulated experimental data provides limited insight into the nature of the size distribution of powders, limited information on size distribution, hence hinders our ability to control the processing parameters. Therefore, interpretation of experimental data in powder size distribution analysis, such as sieving data, generally involves graphical representation.

Table 1. Cumulative weight undersize as a function of powder size [10].

opening (μm)	212	180	150	125	106	90	75	63	53	45	38
weight undersize (g)	129.8	128.7	125.7	117	103.8	87.3	66.5	48.5	31.6	18	7.2

The reliability of graphical representation results depends on the suitability of the procedures used to obtain and to present the experimental data. A standard procedure has been established to obtain the experimental data in powder size distribution analysis (MPIF standard 05 and ASTM standard B214-92). The procedure to present and then interpret the experimental data, on the other hand, is far from complete. The purpose of this paper is to demonstrate that there are several serious shortcomings associated with the conventional procedure, and to formulate a new procedure for presenting the experimental data.

CHAPTER 2. OVERVIEW

It is helpful to describe, at first, the graphical representations generally employed in practice, and the most widely used logarithmic-normal size distribution, before proceeding to address the problems associated with the conventional procedure in graphical representations.

2.1. Graphical representations

Graphical representations of experimental data in powder size distribution analysis include [1]:

1). histograms —— presenting frequency of occurrence versus size range,

2). size frequency curve —— presenting frequency of occurrence as a function of powder size, equivalent to a smoothed-out histogram,

3). cumulative plot —— presenting percent of powders greater (or less) than a given powder size as a function of powder size, and

4). probability paper plot —— essentially the same as cumulative plot, except that the percentage is presented on a probability scale.

2.2. Logarithmic-normal distribution

A logarithmic-normal distribution is closely related to the graphical representation of sieving data. It is commonly found that collections of atomized powders obey log-normal size distribution statistics. Accordingly, there are normally two main objectives of a graphical representation: to determine whether the sieving data obeys log-normal distribution or not, and, if it does, to determine the parameters characterizing a log-normal distribution.

For powders obeying a log-normal distribution in terms of a weight-size relationship, the probability density, $P(D)$, corresponding to powder size D is given by [1-3]:

$$P(D) = \frac{1}{D}\frac{1}{\sigma\sqrt{2\pi}} exp[-\frac{(\ln D - \ln D_m)^2}{2\sigma^2}] \qquad (1),$$

and

$$\int_0^\infty P(D)dD = 1 \qquad (2),$$

where D_m is the mean mass powder diameter, σ is the standard deviation. The probability density, $P(D)$, corresponding to a powder size D is defined as

$$P(D)=\Delta W_p/\Delta D \quad (3),$$

where ΔW_p is the weight percentage of powders with size falling in the range between D and $D+\Delta D$.

It is evident from equation (1) that powders obeying log-normal distributions may be characterized by two parameters, the standard deviation, σ, and the mass mean droplet size, D_m. In practice, another three parameters are also frequently utilized to characterize the powder size distribution. The three parameters are the characteristic powder sizes, d_{16}, d_{50}, and d_{84}, under which *16*, *50*, and *84 wt.%* of powders, respectively, are smaller than the stated sizes. These two characterizing methods are equivalent to each other, since

$$D_m = d_{50} \quad (4),$$

and

$$\sigma = ln(d_{50}/d_{16}) = ln(d_{84}/d_{50}) \quad (5).$$

Graphically, d_{16}, d_{50}, and d_{84} may be determined from a cumulative plot or a probability paper plot, and σ and D_m may be determined from a size-frequency plot. It is worth noting that the magnitudes of these characteristic parameters may be determined graphically either with or without rigorous curve fitting involved. Without curve fitting, however, the nature of powder size distribution is generally unknown. In this case, the characteristic parameters determined are of no physical significance. In addition, even when the nature of size distribution is pre-known, curve fitting is necessary to minimize the extensive experimental errors normally associated with sieving analysis. Therefore, graphical determination of these parameters should be proceeded by curve fitting of experimental results.

2.3. Curve fitting in graphical representations

All of the graphical representations involve the weight percentage, rather than weight, as evident from section 2.1. Conversion of experimentally determined absolute weight into weight percentage necessitates the knowledge of the total weight of the powders under analysis. As will be shown in sections 3 and 4, this parameter is generally unknown. Actually, it is this fact that complicates the procedure of graphical representation. In this

section, the total weight of the powders is temporarily assumed to be a known parameter for the convenience of discussion. In this case, both the weight and weight percentage are readily used in graphical representations and curve fitting.

2.3.1. Histogram and size frequency curves

In these two plots, curve fitting may be established using equation (1). In sieving experiments, however, the direct experimental data are weight (or weight percentage) in a size range, or cumulative weight (or weight percentage) of powders under a given size, as shown in Table 1. In order to obtain the probability density, $P(D)$, equation (3) has to be used. However, this may introduce extensive additional errors into the experimental data by either of the following two ways. First, if the size interval, ΔD, in equation (3) , is selected as the same as that in sieving analysis (for example in Table 1, they are *32, 30, 25, ...*, 8, and *7* μm in decreasing sequence), ΔD is generally too large to be used to accurately calculate $P(D)$ through equation (3). If the size interval, ΔD, in equation (3), is selected to be a smaller value, on the other hand, such as in the range of *1~2* μm, subjective interpolation between the experimental data points would definitely be involved, introducing unexpected errors. Therefore, curve fitting in either histogram or size frequency curve plots would not be considered in the present study.

2.3.2. Cumulative plot

Using equation (1), the cumulative percentage, $C_p(D)$, under size D may be calculated as:

$$\begin{aligned} C_p(D)\% &= \int_0^D P(D)dD \\ &= \int_{-\infty}^{\ln D} \frac{1}{\sigma\sqrt{2\pi}} exp[-\frac{(\ln D - \ln D_m)^2}{2\sigma^2}]d\ln D \\ &= \frac{1}{\sqrt{\pi}} \int_{-\infty}^{\frac{\ln D - \ln D_m}{\sqrt{2}\sigma}} exp[-t^2]dt \\ &= \frac{1}{\sqrt{2\pi}} \int_{-\infty}^{\frac{\ln D - \ln D_m}{\sigma}} exp[-t^2/2]dt \end{aligned} \qquad (6).$$

In sieving analysis, powders may be directly characterized by cumulative weight under size as a function of powder size. When the total weight of the powders is known, then the cumulative weight percentage under size as a function of powder size, $C_p(D)$, may be readily obtained. Accordingly,

equation (6) may be employed to curve fit the experimental data. Unfortunately, the form of equation (6) is so complex such that no attempt was found in the literature to use it to curve fit the experimental data.

2.3.3. Probability paper plot

By defining a function $y=norm(x)$, for which y and x satisfy

$$x\% = \frac{1}{\sqrt{2\pi}} \int_{-\infty}^{y} exp(-t^2/2)dt \qquad (7),$$

equation (6) may be rearranged as

$$\frac{lnD - lnD_m}{\sigma} = norm(C_p) \qquad (8),$$

or

$$\log D = \log D_m + 0.434\sigma \cdot norm(C_p) \qquad (8').$$

In a probability paper plot, the abscissa is the powder size, generally in logarithmic scale, $logD$, while the ordinate is the cumulative weight percentage undersize in probability scale. It is worth noting that the probability scale is calculated using $y=norm(x)$, or equation (7), i.e., $x=50$ corresponds to $y=0$; $x=60$ corresponds to $y=0.25$; $x=90$, $y=1.28$; $x=100$, $y=\infty$; $x=40$, $y=-0.25$; $x=0$, $y=-\infty$; and so on... [4], as shown in Figure 1. Therefore, equation (8), which indicates that $logD$ is a linear function of $norm(C_p)$, predicts a straight line for powders obeying log-normal distributions when the cumulative percentage undersize, C_p, is graphed versus the powder size, D, in a probability paper plot. This feature is well-known and extensively utilized to determine whether a collection of powders obeys a log-normal distribution or not, although its origin is not necessarily always well understood by the user.

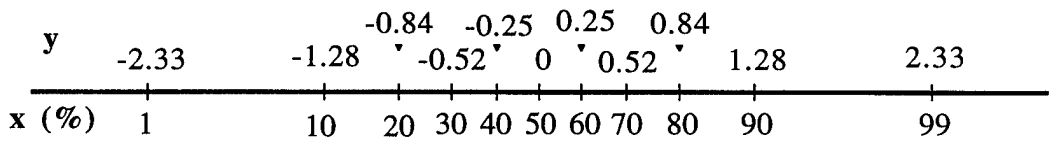

Figure 1. Probability scale y=norm(x).

CHAPTER 3. PROBLEMS ASSOCIATED WITH GRAPHICAL REPRESENTATION PROCEDURE

In this section, the problems associated with graphical representation procedures will be discussed. Essentially, all of these problems originate from the fact that the total weight of powders is generally unknown, which is closely related to the removal of coarse/fine powders in practical atomization experiments.

3.1. Removal of coarse/fine powders

It is evident from section 2.1 that all of the graphical representations involve weight percentage (or frequency), rather than the absolute weight. However, experimental data generally involve absolute values. Therefore, the first step of graphical representation is to convert the absolute weight, in the case of sieving experiments, into weight percentage. This necessitates the knowledge of the total weight for the powders under analysis. Unfortunately, this parameter is generally unknown in a lot of pratical situations. This may appear unusual; however, any detailed examination of the powder size distribution analysis will indicate that this is generally beyond the capability of typically used experimental arrangements. Suffice it to point out here that the powders subjected to experimental size distribution analysis, such as sieving, are different from the powders formed because of dust separation by cyclones or/and removal of coarse particles. To make this point more clear, let us consider a dispersion of powders observing log-normal distribution, as shown in Figure 2. Dust separation by cyclones and removal of coarse particles truncate the two tails from the bell shape distribution in Figure 2 by introducing two size-limits, D_{min}, the lower limit, and D_{max}, the upper limit. While the total weight of the truncated distribution may be readily measured experimentally, the total weight of powders used for conversion from weight into weight percentage in a graphical representation of sieving data should be that of the entire powders, rather than the truncated one. Nevertheless, it is impossible to experimentally measure the total weight of the entire distribution of powders, since, by definition, the powder size ranges from zero to infinity for a log-normal distribution.

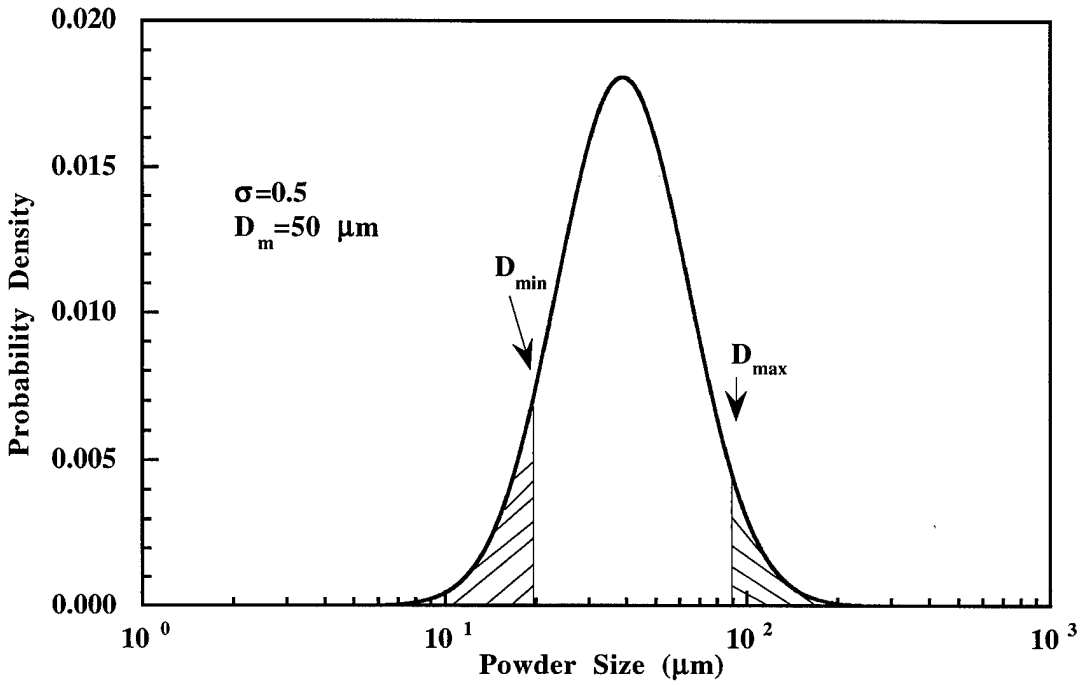

Figure 2. Schematic graph showing probability density, P(D), as a function of the powder size for a collection of log-normally distributed powders.

Removal of coarse/fine powders, or the difficulty in determining the total weight of powders experimentally, is not the problem associated with size distribution analysis. Actually, it is consistent with the basic concept to explore the real size distribution from limited experimental data [1]. The question is how to analyze the experimental data to minimize the effect of the intrinsic experimental difficulties on the final results. This is crucial to ensure that the final results are reliable and of significance. The conventional graphical representation procedure, however, hardly addressed this issue, as shown below.

3.2. Substitution by truncated distribution

In a conventional procedure, the weight of a truncated distribution is generally employed as a substitution, for the purpose of conversion from weight into weight percentage, of the total weight of the powders. This substitution might be an acceptable approximation when the weight of the tails is insignificant relative to that of the entire distribution. As the tails become comparable to the central portion in terms of weight, the error

resulting from this approximation may be large. The problem is complicated, however, by the fact that the relative contribution of the tails to the entire distribution, i.e., the criterion for the accuracy of the approximation, generally remains unknown until the total weight of the entire powders is determined.

The conventional procedure is also flawed as a result of another factor. By assuming the weight of a truncated distribution as the total weight of the entire distribution, the experimentally obtained absolute weight may be readily converted into weight percentage. However, a natural result of this assumption is that the cumulative percentage undersize corresponding to D_{max} is *100%*. Since it is impossible to graph *100%* in a probability paper plot, this data point is then ignored. This treatment is difficult to be justified, but widely employed.

3.3. Reliability

In the literature, an implicit concept that is widely used involves the assumption that, if the data points obey a log-normal distribution, then the results are reliable. To examine its validity, the experimental data in Table 1 were analyzed using the conventional procedure, with the results shown in Figures 3(a) through (d). The upper limit of powder size, D_{max}, was chosen to be *212, 150, 90,* and *63* μm in Figures 3(a), 3(b), 3(c), and 3(d), respectively. The magnitude of D_{min} was temporarily set to be zero for all cases, as normally treated in conventional procedures. Accordingly, the size range of the truncated distributions are *0~212* μm, *0~150* μm, *0~90* μm, and *0~63* μm for Figures 3(a) through (d), respectively. Moreover, from Table 1, the weight of these truncated distributions are *129.8, 125.7, 87.3,* and *48.5* g for Figures 3(a) through (d), respectively. The data were graphed on probability paper plot and curve fitted, with the fitting coefficient, along with the characteristic parameters, summarized in Table 2. It is evident from Figure 3 and Table 2 that introducing different upper limits of powder size, D_{max}, does not affect the nature of the size distribution; the data consistently followed log-normal distribution. The characteristic parameters, however, vary extensively with D_{max}, rather than remain unchanged, as evident from Table 2. It is important to recall that the ultimate purpose of size distribution analysis is to determine the real size distribution, and the characteristic parameters for the real size

distribution of the powders under analysis are unique. Therefore, at least some of the results in Table 2 provide misleading information as to the characteristics of the real size distribution. This conclusively reveals that data points obeying log-normal distribution alone cannot ensure the reliability of the results obtained.

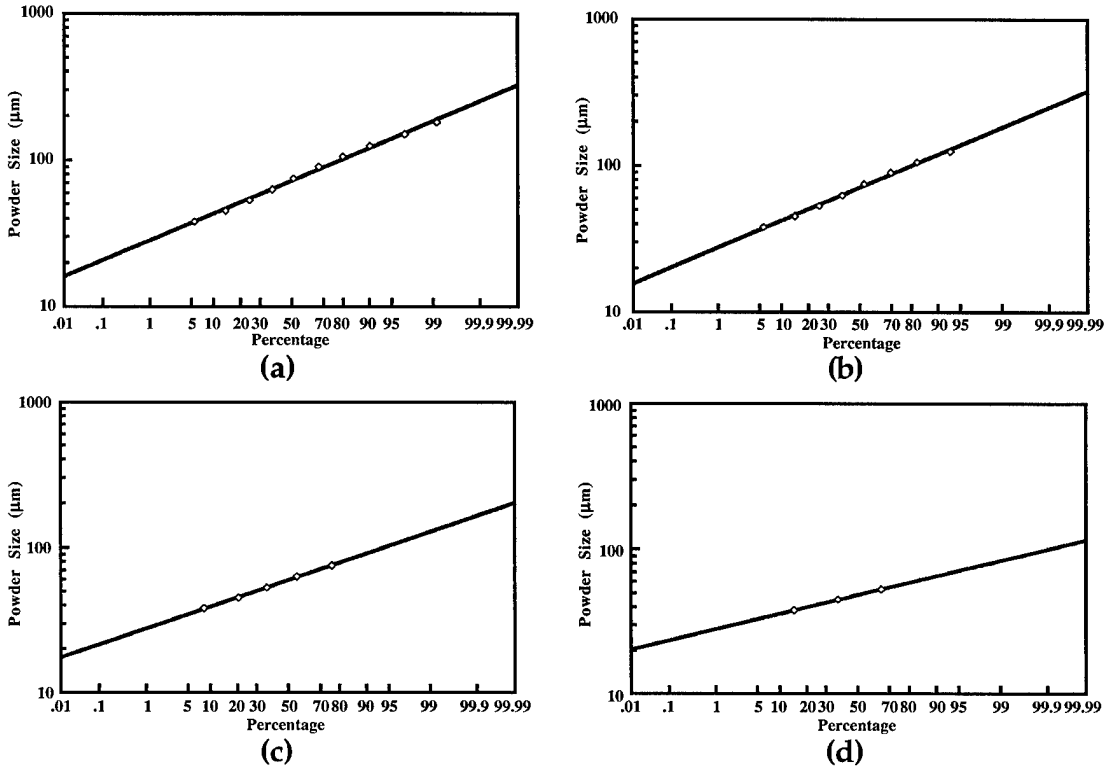

Figure 3. Probability paper plots for data in Table 1, using conventional procedure, with various D_{max} introduced: (a) D_{max}=212 μm; (b) D_{max}=150 μm; (c) D_{max}=90 μm; and (d) D_{max}=63 μm.

Table 2. Characteristic parameters and fitting coefficients obtained using the conventional procedure for data in Table 1 with different D_{max}(μm) introduced.

parameters	d_{16} (μm)	d_{50} (D_m) (μm)	d_{84} (μm)	σ	fitting coefficient
D_{max}=212	48.26	72.21	108.05	0.403	99.703%
D_{max}=150	47.37	71.09	106.69	0.406	99.713%
D_{max}=90	42.88	59.59	82.81	0.329	99.952%
D_{max}=63	38.40	48.47	61.19	0.233	99.996%

3.4. Difficulty in determining reliability

Since there are several difficult-to-be-justified assumptions associated with the conventional procedure, no attempt will be made here to solve, or to prove it is impossible to solve, the reliability problem under the framework of conventional graphical representation procedure. Suffice it to point out that the problem is complicated by the intrinsic difficulty in using a probability paper plot. This may be briefly described as follows. Considering the bell shape for a log-normal distributed collection of powders in Figure 2, as D_{max} increases, the results are expected to gradually approach that of the real size distribution, becoming more and more reliable. This feature might enable one to judge the reliability of the results obtained. Unfortunately, this idealized situation is rarely realized in a probability paper plot. As D_{max} deviates from the mean mass diameter, D_m (which means D_{max} increases), the experimental error in the data points will be more and more exaggerated, such that a minor experimental error associated with the data points corresponding to large D values would completely change the final results [5]. This could only be avoided by having the data points *"weighted"* (i.e., evaluating the importance of the data points) before graphical representation, as discussed in detail in reference [5]. Calculation and assignment of the *"weight"* for each data point, however, requires a knowledge of the weight percentage corresponding to each data point, which necessitates a knowledge of the total weight of the powders [5]. In the conventional procedure, the total weight of the powders is substituted using the truncated distribution. The appropriateness of this substitution is, in turn, determined by the reliability of the results obtained.

3.5. Artificial distribution

The effect stemming from removal of coarse/fine powders on the final results was addressed by Irani [1, 6] from another point of view. According to Irani [1, 6], because of the removal of coarse/fine powders, the data points in a probability paper plot asymptotically approach a line parallel to the abscissa (the probability scaled axis), rather than fall onto a straight line as expected. To eliminate or minimize the effect of removal of coarse/fine powders, Irani [1, 6] suggested that the total weight should be a value greater than the weight of the corresponding truncated distribution. To determine this value, a

reiteration method is employed: assuming a total weight, converting weight into weight percentage based on the assumed total weight, then graphing the converted weight percentage on a probability paper plot versus powder size, and assuming a new total weight.....and so on, until the data graphed on the probability paper plot satisfactorily fall onto a straight line.

This method, however, has three drawbacks. Firstly, as discussed in section 3.3, data points falling onto a straight line alone does not ensure that the results are reliable. Although the discussion in section 3.3 is under the assumption that the total weight of powders may be substituted by that of the truncated distribution, it is generally true that data points obeying log-normal distribution alone does not assure the reliability of the results, as will be shown in section 4.4. Secondly, the intrinsic difficulty associated with probability paper plot cannot be solved using this method, and hence still affects this method. Finally, this method failed to formulate any equations in determining the total value of powders from curve fitting the experimental data, rendering the entire procedure dubious.

CHAPTER 4. PROPOSED APPROACH

As evident from the above discussion, along with several implicit, hard-to-be-justified, assumptions, the conventional graphical representation procedure failed to address the reliability of its results. In the following sections, a new procedure will be formulated. The proposed procedure is capable of extracting the total weight of powders from experimental data, of determining the nature of size distribution, of characterizing the characteristic parameters, and simultaneously, of determining the reliability of its results.

4.1. Effect of removal of coarse powders

In this section, with D_{min} being temporarily set to be zero, only the effect of D_{max} will be considered. The effect of introducing the lower limit of powder size into the distribution will be discussed in section 4.2.

4.1.1. Mathematical formulation

Equations (1)-(8) correlate powder size with probability (equation (1)), or cumulative weight percentage under size (equations (6) and (8)). Experimental data, however, are absolute weight and powder size (refer to Table 1). This necessitates development of equations directly correlating the powder size with the absolute weight. The development of these equations may be readily accomplished by incorporating the total weight of powders into the analysis in equations (1)-(8).

Assuming the total weight to be W_t, the cumulative weight percentage undersize D may be calculated as

$$C_p(D)\% = W_{under}(D)/W_t \qquad (9),$$

where $W_{under}(D)$ is the cumulative weight undersize D. When $D_{min} = 0$, $W_{under}(D)$ is equivalent to the experimentally obtained cumulative weight undersize, $W^E_{under}(D)$. Substituting equation (9) into equation (8) yields

$$\log D = \log D_m + 0.434\sigma \cdot norm(100\frac{W^E_{under}(D)}{W_t}) \qquad (10).$$

Similarly, substituting equation (9) into equation (6) gives:

$$W^{E}_{under}(D) = W_t \frac{1}{\sqrt{2\pi}} \int_{-\infty}^{\frac{\ln D - \ln D_m}{\sigma}} exp(-t^2/2)dt \qquad (11).$$

When the total weight is known, equations (10) and (11) are essentially equivalent to equations (6) and (8). In this case, development of equations (10) and (11) is of little significance. When the total weight is unknown, however, these two sets of equations are totally different. While equations (6) and (8) may not be utilized to curve fit the experimental data (absolute value), equations (10) and (11) can. More importantly, equations (10) and (11) enables extraction of the unknown total weight of powders, W_t, by curve fitting the sieving experimental data.

4.1.2. Selection of governing equation for curve fitting

In the last section, two equations were developed to correlate the powder size with the cumulative weight undersize: equation (10) which curve fits D as a function of $W^{E}_{under}(D)$; and equation (11) which curve fits $W^{E}_{under}(D)$ as a function of D. Mathematically, equation (10) is equivalent to equation (11). However, experimental data is unavoidably associated with some errors, making these two equations different from each other in terms of curve fitting. In the present study, equation (11) is uniquely selected to be the governing equation in curve fitting because of the following two reasons.

Firstly, in curve fitting, if the governing equation is selected to be $y=f(x)$, then it is generally assumed that the independent variable, x, is known to be without error [7]. All the errors are in the dependent variable y [7]. In a sieving experiment, the powder size D is generally predetermined, i.e., free of error. The experimental error normally arises from the measurement of the cumulative weight undersize $W^{E}_{under}(D)$. Accordingly, compared with equation (10), equation (11), which expresses $W^{E}_{under}(D)$ as a function of D, is more suitable to be employed as the governing equation.

Secondly, in curve fitting, it is generally assumed that the errors associated with the dependent variable, y, are random [7]. In a sieving experiment, the error arising from the measurement of the cumulative weight undersize may be reasonably taken to be random. Therefore, selecting equation (11) as the governing equation is consistent with the above assumption in curve fitting.

If equation (10) is used, on the other hand, $W^E_{under}(D)$ would be taken as without error. Instead, any errors arising from $W^E_{under}(D)$ would be evaluated in terms of D. This makes the error no longer random, as elucidated as follows. It is evident from Figure 1 that , as $x\%$ deviates gradually from 50%, $y=norm(x)$ increases (positive) or decreases (negative) more and more rapidly. Suppose there is a deviation Δx in the independent variable x, the corresponding deviation in y would depend on the value of x. Let the deviation in y be $\Delta y \mid_{50}$ for $x\%=50\%$, it would become $15\Delta y \mid_{50}$ if $x\%=99\%$ (or 1%), and $28\Delta y \mid_{50}$ if $x\%=99.5\%$ (or 0.5%), and so on, progressively [5]. The situation discussed here applies to equation (10) by simply substituting $(\log D - \log D_m)/0.434\sigma$ as y, and $100W^E_{under}(D)/W_t$ as x. If any errors originating from $100W^E_{under}(D)/W_t$, or from $W^E_{under}(D)$, are evaluated in terms of $(\log D - \log D_m)/0.434\sigma$, or D, the results would be dependent on the magnitude of $100W^E_{under}(D)/W_t$. The larger $100W^E_{under}(D)/W_t$, the larger the error. Accordingly, if the errors in $100W^E_{under}(D)/W_t$ or $W^E_{under}(D)$ are random, the evaluated errors in terms of $(\log D - \log D_m)/0.434\sigma$, or D, would no longer be random. In this case, the experimental point should be *"weighted"* (i.e., evaluating the importance of the data points) before curve fitting [5, 7]. Calculation and assignment of the *"weight"* for each data points, however, requires the knowledge of the weight percentage corresponding to each data point, which necessitates the knowledge of the total weight of the powders [5]. Unfortunately, the latter, i.e., the total weight of the powders, is a variable to be determined, making the assignment of the weight impossible.

Finally, a remark should be made regarding the conventional probability paper plot. Since one axis of this plot is in probability scale, which is $y=norm(x)$, the error would be analyzed in terms of D, or $norm[100W^E_{under}(D)/W_t]$, rather than $100W^E_{under}(D)/W_t$, or $W^E_{under}(D)$. Accordingly, curve fitting in probability paper plot always encounters the problem associated with equation (10). This is the reason behind the intrinsic difficulty in the probability paper plot approach mentioned earlier.

4.1.3. Realization of curve fitting

It is evident that equation (11) is, at least, as complex as equation (6). The practical usefulness of equation (11) relies on the availability of a quick and

effective method to curve fit the experimental data using this equation. This may be realized in a KaleidaGraph software (version 3.0 or above). In the KaleidaGraph, there are two normal distribution related functions available: $y=norm(x)$ and $y=inorm(x)$. Function $y=norm(x)$ was discussed earlier. Function $y=inorm(x)$ is related to equation (11) as follows:

$$inorm(x) = \frac{100}{\sqrt{2\pi}} \int_{-\infty}^{x} exp(-t^2/2)dt \qquad (12),$$

which transforms equation (11) into:

$$W_{under}^{E}(D) = \frac{1}{100} W_t inorm[\frac{1}{\sigma} ln(\frac{D}{D_m})] \qquad (13).$$

Governing equation (13) may be defined under the General Curve Fitting menu in KaleidaGraph Window. To ensure the definition being complete, the partial derivative of equation (13) relative to W_t, σ, and D_m, should be given. This may be readily accomplished if one notices that

$$\frac{\partial inorm(x)}{\partial x} = \frac{100}{\sqrt{2\pi}} exp(-\frac{x^2}{2}) \qquad (14).$$

4.1.4. Applications

Six sets of sieving data (Tables 1 and 3) from different sources were analyzed using the formulated procedure, with special attention to its capability of providing reliable results.

Figure 4 shows the results for the data in Table 1 with D_{max}=*212* μm, which is the D_{max} employed in the experiment. It is evident there that the experimental data obeys the log-normal distribution. The total weight extracted is *132.0 ± 1.0* g, with σ=*0.449 ± 0.010* and D_m=*74.0 ± 0.6* μm (Table 4). The results, including W_t, σ, d_{50} (D_m), the standard errors associated with each of them, and the fitting coefficient, obtained for the data in Table 3 with D_{max} equal to the value employed in each experiments, which are *600, 425, 125, 250,* and *250* μm for the data in columns A, B, C, D, and E of Table 3, respectively, were also provided in Table 4.

It is of interest to note that the total weight, W_t, extracted (Table 4) for the data in columns A and B, which are *1661.1* and *127.6* g, respectively, are smaller than the experimentally measured cumulative weight undersize D_{max}, which are *1667.6* and *129.52* g for columns A and B in Table 3, respectively. This may

be understood as follows. According to Figure 2, as the powder size increases to be much larger than D_m, the cumulative weight undersize, $W^E_{under}(D)$, is expected to approach, but always remain smaller than, W_t. However, the experimental data is always associated with some errors, which makes $W^E_{under}(D)$ smaller or larger than the value it is supposed to be in the idealized

Table 3. Experimental sieving data to be analyzed.

opening (μm)	Cumulative Weight Undersize (g)				
	A	B	C	D	E
600	1667.6	--------	------	-----	----
425	1656.3	129.52	------	-----	----
300	1642.6	--------	------	-----	----
250	1630.7	128.25	------	100	101
180	1578.0	127.11	------	-----	----
150	1509.9	126.63	------	-----	----
149	-------	--------	------	59.0	95.6
125	1392.7	126.13	678.6	-----	----
106	1172.2	125.56	619.7	-----	----
105	--------	--------	------	41.1	87.3
90	775.84	124.66	561.5	-----	----
75	608.76	121.82	512.3	-----	----
74	--------	--------	------	27.9	75.8
63	374.38	111.12	341.7	24.5	70.9
53	277.54	86.27	243.5	-----	----
45	142.95	68.961	195.1	-----	----
44	--------	--------	------	12.2	52.9
38	67.67	44.876	56.8	-----	----
source	[11]	[12]	[13]	Run 73N [14]	Run 69N [14]

situation. Consequently, when $W^E_{under}(D)$ is very close to W_t, any minor experimental error may raise $W^E_{under}(D)$ to exceed W_t. It is worth noting that this type of experimental error could never be tolerated by equation (10), as explained as follows. The first step of curve fitting using equation (10) is to calculate $norm[100W^E_{under}(D)/W_t]$ as a function of the independent variable

$W^E_{under}(D)$. Function $norm[100W^E_{under}(D)/W_t]$, by definition, requires $W^E_{under}(D)/W_t$ to be smaller than 1, i.e., $W^E_{under}(D)<W_t$. When $W^E_{under}(D)>W_t$ overflow would occur, and the curve fitting would be terminated. This further demonstrates that equation (10) is only of theoretical significance.

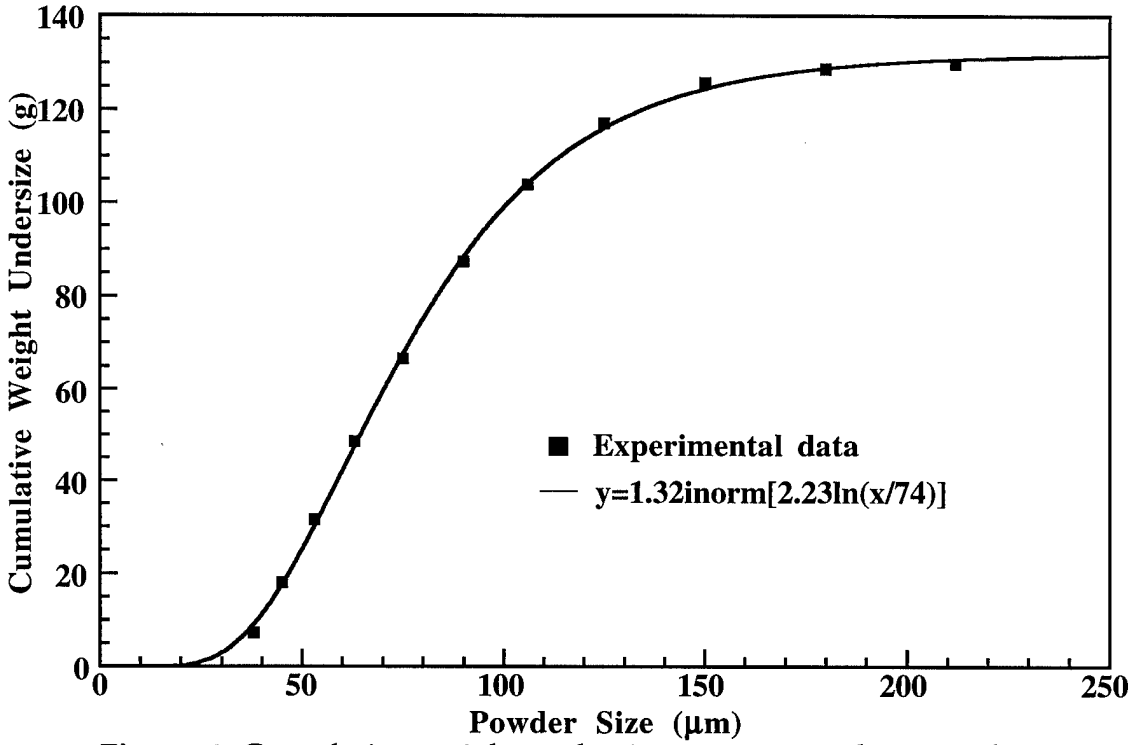

Figure 4. Cumulative weight undersize versus powder size plot for the data in Table 1 using the newly formulated procedure. The D_{max} is set to be equal to that employed in the experiment.

Table 4. Characteristic parameters and fitting coefficients obtained using equation (13) for data in Tables 1 and 3 with D_{max}(μm) equal to that employed in experiment.

parameters		W_t	d_{50} (D_m)	σ	fitting
Data	D_{max}	(g)	(μm)		coeff. (%)
table 1	*212*	132.0 ± 1.00	74.0 ± 0.6	0.449 ± 0.010	99.971
A, tab. 3	*600*	1661.1 ± 23.6	86.5 ± 1.6	0.435 ± 0.024	99.754
B, tab. 3	*425*	127.6 ± 0.8	43.7 ± 0.4	0.351 ± 0.017	99.778
C, tab. 3	*125*	696.5 ± 43.0	61.3 ± 2.9	0.411 ± 0.057	99.363
D, tab. 3	*250*	1301.3 ± 2358.7	4431.3 ± 13022	2.014 ± 0.703	99.907
E, tab. 3	*250*	103.0 ± 1.2	42.3 ± 0.7	0.866 ± 0.044	99.932

Table 5. Characteristic parameters and fitting coefficients obtained using equation (13) for data in Tables 1 and 3 with different D_{max}(μm) introduced. D_{min} is assumed to be zero in all cases.

parameters		W_t	error	d_{50} (D_m)	error	σ	error	fitting
Data	D_{max}	(g)	(%)	(μm)	(%)		(%)	coeff. (%)
	212	132.0	0.8	74.0	0.8	0.449	2.2	99.971
table 1	*150*	134.8	1.6	75.1	1.3	0.462	2.9	99.971
	90	118.7	8.9	69.6	5.3	0.418	8.4	99.937
	63	74.3	11.3	56.0	4.7	0.304	9.4	99.981
	600	1661.1	1.4	86.5	1.8	0.435	5.5	99.754
	300	1660.3	2.2	86.5	2.3	0.435	6.7	99.702
table 3	*180*	1719.9	5.5	88.7	4.5	0.458	10	99.621
col. A	*125*	2955.8	41	129.8	31	0.646	21	99.681
	90	1195.8	26	75.6	15	0.444	20	99.718
	63	454.2	15	49.9	5.8	0.246	20	99.826
	425	127.6	0.6	43.7	0.9	0.351	4.8	99.778
	250	127.3	0.7	43.6	0.9	0.348	4.9	99.793
table 3	*150*	127.0	1	43.6	1.1	0.346	5.8	99.776
col. B	*90*	129.5	3.2	44.0	2	0.363	10	99.73
	*63**	166.6	40	51.1	26	0.497	40	99.76
	*53**	99.5	∞	39.3	∞	0.270	∞	100
table 3	*125*	696.5	6.2	61.3	4.7	0.411	14	99.363
col. C	*90*	667.3	20	59.7	12	0.387	29	98.89
	*63**	367.3	30	46.2	12	0.232	59	98.075
table 3	*250**	1301.3	180	4431.3	290	2.014	35	99.907
col. D	*149**	147.1	73	198.9	94	1.129	36	99.781
73N	*105**	61.0	38	77.4	35	0.688	36	99.698
table 3	*250*	103.0	1.2	42.3	1.7	0.866	5.1	99.932
col. E	*149*	102.4	3	42.1	2.9	0.852	9.5	99.903
69N	*105*	97.3	5.9	40.4	4.7	0.762	16	99.897

In order to investigate the capability of determining the reliability of the results, a method similar to that in section 3.3 was employed, i.e., introducing different D_{max}. The results are summarized in Table 5. As evident from Table 5, the characteristic parameters obtained are, in general, a function of D_{max}.

This again raises the question: when would the results be reliable. It is evident from Table 5 (the fitting coefficient column) that introducing different D_{max} does not affect the nature of size distribution, i.e., in all cases, the data points obey log-normal distribution. This suggests that, under the newly formulated procedure, the reliability of the results may not be determined by the nature of size distribution either, similar to the situation encountered under the conventional framework as discussed in section 3.3. However, there are two ways to evaluate the reliability of the results under the newly formulated procedure.

The reliability of the results may be evaluated, to some extent, by the standard errors associated with the characteristic parameters determined. When the standard error is very large, such as *30%* or above, it is highly unlikely that the results are reliable. When the standard error is very small, such as *1%* or less, it is reasonable to take the results as reliable. With this criterion, several sets of results, which were marked by asterisks, in Table 5 may be readily determined to be unreliable. Nevertheless, it is impossible to provide a number to unambiguously judge the results: when the error is above it, the result is unreliable; otherwise, reliable. Accordingly, when the standard error is moderate, such as *5~15%*, it is difficult to conclusively determine the reliability of the results using this method.

A more effective but somewhat time-consuming way relative to the method mentioned above is associated with the intrinsic feature of the log-normal size distribution. For a collection of powders obeying log-normal distribution, as D_{max} increases further and further, the cumulative weight would finally tend to flatten off (refer to Figure 4). Once this region is reached, any further increases in D_{max} would have only slight effect on the cumulative weight. Consequently, the results obtained are expected to be close to each other thereafter. Accordingly, if the results, which are W_t, σ, and d_{50} (D_m) in the present study, corresponding to the introduced D_{max} were plotted as a function of D_{max}, it is anticipated that all of the curves representing each of the characteristic parameters would flatten off at certain $D_{max} = D^f_{max}$. If D^f_{max} is smaller than the D_{max} employed in the experiment, the flattened regions may be observed; and hence the results obtained may be reliable. Otherwise,

the flattened regions would be absent, and the results would be thought unreliable. With this criterion, the reliability of the results may be evaluated.

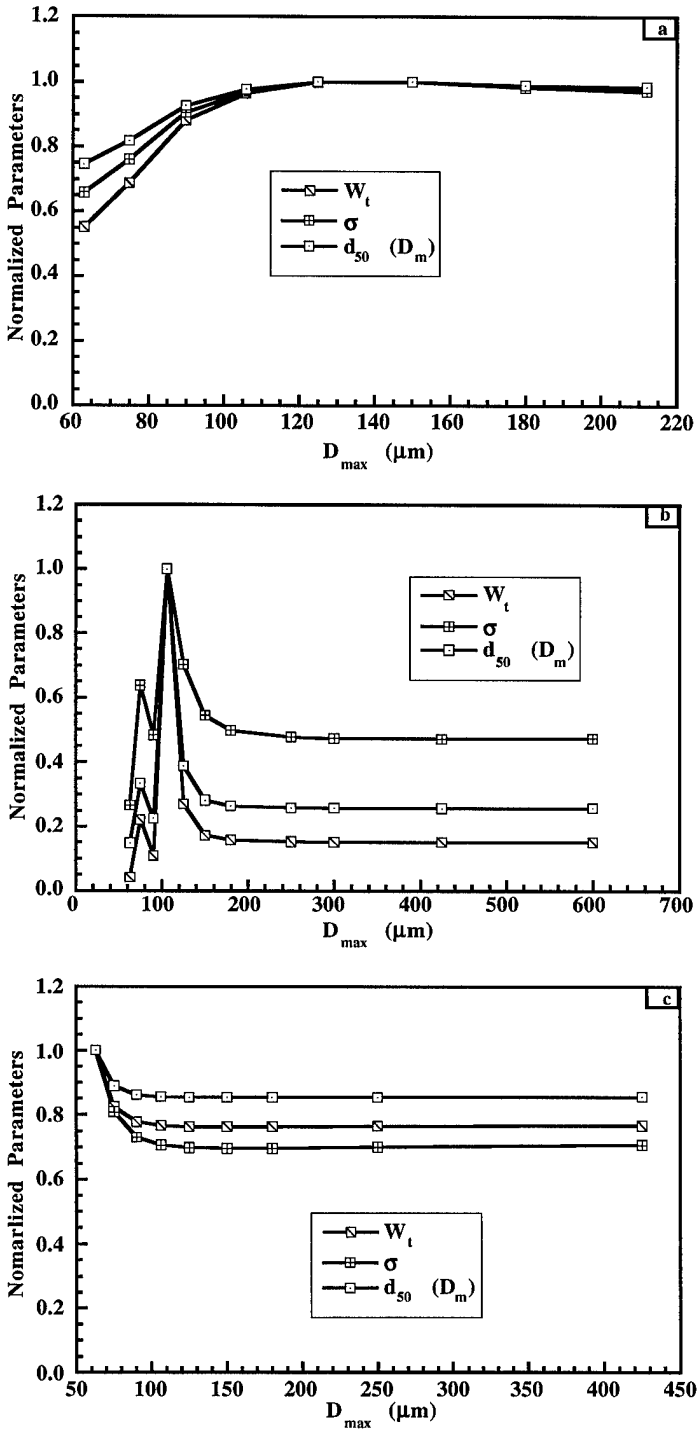

Figure 5. The characteristic parameters (normalized) obtained under different introduced D_{max} for data in Table 1 (a), columns A (b), B (c), C (d), D (e), and E (f) of Table 3.

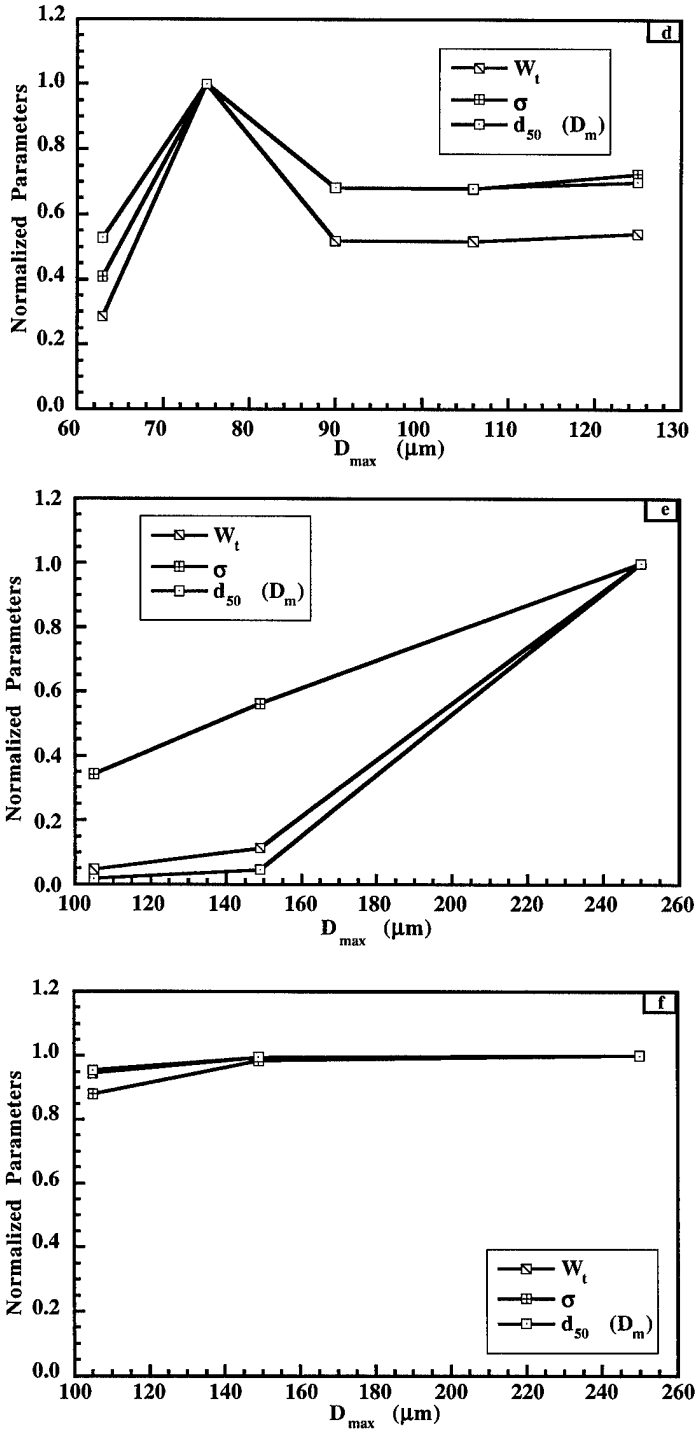

Figure 5 (continued). The characteristic parameters (normalized) obtained under different introduced D_{max} for data in Table 1 (a), columns A (b), B (c), C (d), D (e), and E (f) of Table 3.

Figures 5(a) through (f) show the obtained results as a function of D_{max} for the six sets of data under analysis. For the convenience of graphical representation, all of the results, for any given set of data, were normalized by their corresponding maximum magnitude. For example, the maximum extracted total weight for the data in column B of Table 3 is *166.6* g, corresponding to an introduced D_{max} of *63* μm. Accordingly, in Figure 5(c), all W_t values were normalized by *166.6* g. It is evident from Figure 5 that, except those in Figure 5(e), all of the curves exhibit a flattened out region as D_{max} increases. Moreover, for each specific set of data, the D_{max} at which the curve begins to flatten is almost the same for all of the three parameters, W_t, σ, and d_{50} (D_m). For example, in Figure 5(c), all of the three parameters tend to be relatively insensitive to the change of D_{max} after D_{max} increases to 90 μm and beyond. The extended flattened regions in Figures 5(a)-(c) suggest that the data corresponding to these figures, which are the data in Table 1, columns A, and B of Table 3, respectively, are highly sufficient to yield reliable results. The limited flattened regions in Figures 5(d) and (f) implies that the results obtained with D_{max} equal to that employed in experiment are almost reliable. In these cases, even though it is not mandatory, more data points, i.e., larger D_{max} employed in the experiment, would be helpful to gain more confidence on the results. The absence of a flattened region in Figure 5(e) indicates that the data in column D of Table 3 are not sufficient to give any reliable results. Finally, it is of interest to note that before the flattened region was reached, the results may monotonously increase (Figure 5(a)) or decrease (Figure 5(c)), or vibrate back and forth (Figure 5(b)).

It is worthwhile to point out that the intrinsic feature of a log-normal size distribution employed to determine the reliability in the above section remains to be the same in the conventional procedure. However, in the conventional procedure, the intrinsic difficulty associated with the probability paper plot makes the utilization of this feature almost impossible, as discussed earlier. As a simple example, the data in column B of Table 3 were analyzed using the conventional procedure. The results were shown in Figure 6. No flattened regions similar to that in Figure 5(b) were observed in Figure 6. As D_{max} increases, the curve corresponding to W_t did flatten off. The curves corresponding to σ and d_{50} (D_m), however, did not flatten off as that of W_t did. Instead, σ keeps increasing, while d_{50} (D_m) gradually decreases.

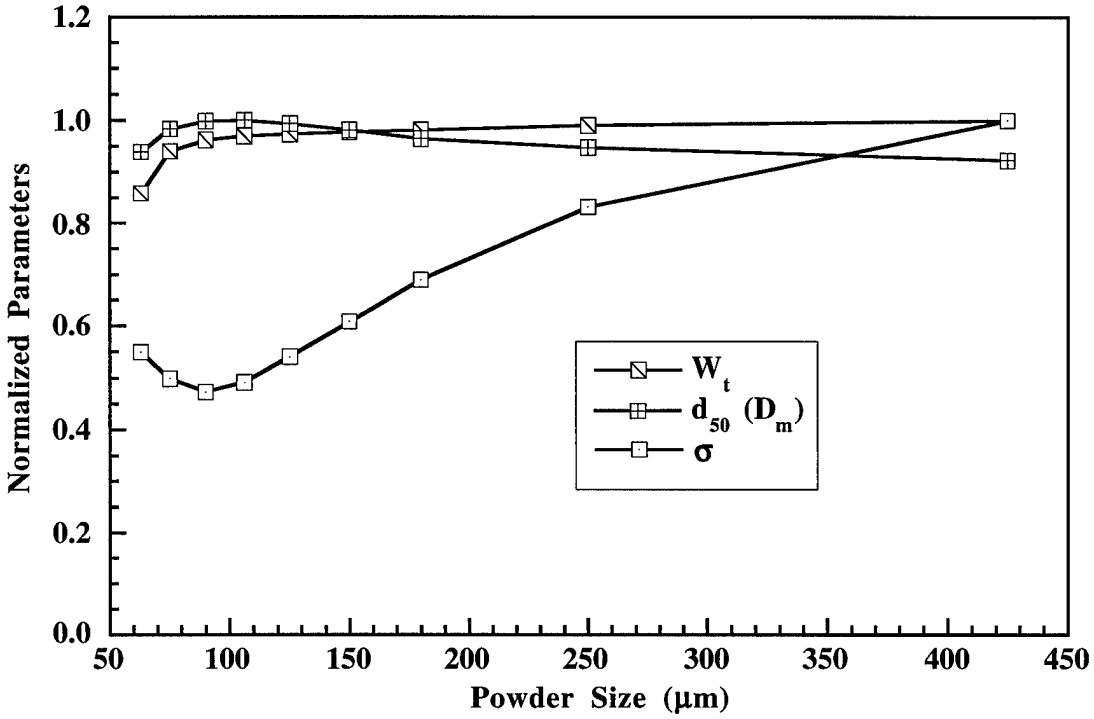

Figure 6. The characteristic parameters (normalized) obtained, using the conventional procedures, for the data in column B of Table 3 as a function of D_{max}.

When the results obtained are determined to be unreliable, such as the case corresponding to the data in column D of Table 3, a larger upper limit of powder size, D_{max}, should be used in the experiment. However, sometime this may be very challenging to be achieved in sieving experiments. The fact that the largest opening in the U.S. standard sieving set is 600 μm limits the availability of sieves with openings larger than 600 μm. Moreover, selection of the upper limit of powder size, D_{max}, in real experiments is generally based on another consideration. In many situations, the spherical powders formed are mixed with irregularly shaped particles such as splats and coalesced particles. It is unsuitable to consider these particles as spherical powders. While complete separation of spherical powders from splats and coalesced powders is almost impossible, it is noticed that the presence of these particle is sparse when the powder size is not too large, and may be neglected. When powder size increases, presence of these particles becomes more frequent. In some cases, before the powder size increases to *600* μm, presence of splats and

coalesced powders becomes so frequent that it can no longer be neglected compared with the total quantity of powders. Accordingly, a value smaller than *600* μm, for example *300* μm, is set to be the upper limit of powder size, below which presence of splats or coalesced powders can be neglected. Following this criterion of selection of D_{max}, it may be unacceptable in some practical situations to raise D_{max} to a value larger than the previously selected one, even though the newly selected value is smaller than *600* μm. In these cases, alternative existing characterization techniques, such as light -scattering, should be employed, or innovative techniques should be explored if meaningful results are anticipated.

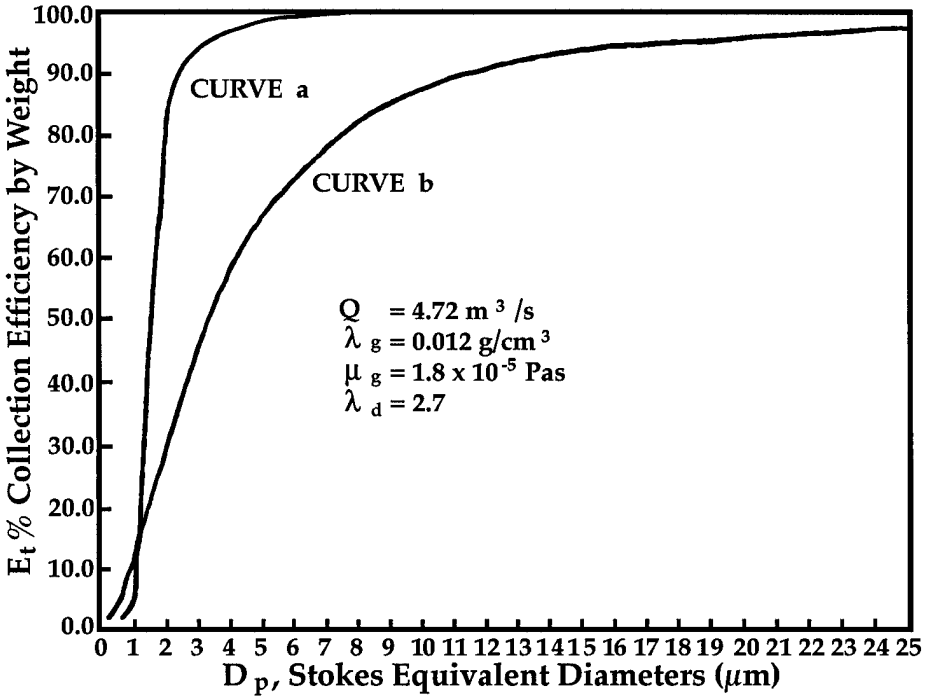

Figure 7. Collection efficiency of a cyclone as a function of powder size for (a) XQ120 cyclone and (b) XQ465 cyclone under identical conditions: gas flow rate (Q), gas density (λ_g), gas absolute viscosity (μ_g), and particle specific gravity (λ_d) [9].

4.2. Effect of dust separation by cyclone

As mentioned earlier, the size distribution of the powders formed initially is generally affected by dust separation, for example in cyclones, which remove some very fine powders. The effect of dust separation by cyclone on the

distribution of the powders is somewhat different from that of the removal of coarse powders. In the removal of coarse powders, the effect is discrete. For example, if the powders are topped using a 425 μm sieve (35 mesh), powders with size larger than 425 μm would be removed, while those with size smaller than 425 μm would be left unaffected. In dust separation by cyclone, the effect is continuous, as shown in Figure 7. Powders with powder size smaller than 1 μm would be almost completely removed. As the powder size increases, the powders would be partially removed, and the percentage being removed would gradually decreases to zero. This continuous feature greatly complicates the problem. To make the problem tractable, a discrete removal, similar to removal of coarse powders, will be assumed. This may be an acceptable assumption if the collection efficiency curve is very steep, such as in Figure 7.

4.2.1. Governing equations

When powders smaller than the lower limit of powder size, D_{min}, are removed, the experimentally obtained cumulative weight undersize, $W^E_{under}(D)$, is nominal (refer to Figure 2). In this case, $W^E_{under}(D)$ is the cumulative weight of powders with size in the range from D_{min} to D, rather than from 0 to D. Therefore,

$$W_{under}(D) = W^E_{under}(D) + W_{under}(D_{\min}) \qquad (15),$$

where $W_{under}(D_{min})$ is the cumulative weight under size D_{min}. The cumulative weight under size D_{min}, $W_{under}(D_{min})$, may be further explicitly expressed, in terms of D_{min}, as follows:

$$W_{under}(D_{min}) = W_t \frac{1}{\sqrt{2\pi}} \int_{-\infty}^{\frac{\ln D_{min} - \ln D_m}{\sigma}} exp(-t^2/2)dt$$

$$= \frac{1}{100} W_t inorm[\frac{1}{\sigma} ln(\frac{D_{min}}{D_m})] \qquad (16).$$

With equations (15) and (16), equations (10) and (13) would take the following form

$$\log D = \log D_m + 0.434\sigma \cdot norm[100 \frac{W^E_{under}(D) + W_{under}(D_{min})}{W_t}]$$

$$= \log D_m + 0.434\sigma \times$$

$$norm\{100 \frac{W^E_{under}(D)}{W_t} + inorm[\frac{1}{\sigma} ln(\frac{D_{min}}{D_m})]\} \qquad (17),$$

and

$$W^{E}_{under}(D) = \frac{1}{100} W_t inorm[\frac{1}{\sigma} ln(\frac{D}{D_m})] - W_{under}(D_{min})$$

$$= \frac{1}{100} W_t \{inorm[\frac{1}{\sigma} ln(\frac{D}{D_m})] - inorm[\frac{1}{\sigma} ln(\frac{D_{min}}{D_m})]\} \qquad (18),$$

respectively.

In selection of the governing equation for curve fitting from equations (17) and (18), arguments similar to those in section 4.1.2 apply here. Moreover, equation (17) is much more complex than equation (18) in terms of computer manipulation. Accordingly, equation (18) is uniquely selected as the governing equation. Its usage in a computer is similar to that discussed in section 4.1.3.

4.2.2. Evaluation of the effect of D_{min}

The lower limit of powder size, D_{min}, is determined by design of the cyclone [8]. It may range from *1* μm to *100* μm, depending on the details of the design [8]. To illustrate its possible effect, D_{min}=*5*, *10*, and *30* μm will be considered in the present study.

The experimental data in Table 1 and in columns A, B, C, and E of Table 3 were analyzed using equation (18), with D_{min} in it set to be *5*, *10*, and *30* μm, and D_{max} equal to the ones employed in each experiment. The results, along with those in Table 4 which correspond to the case with D_{min}=*0* μm, were summarized in Table 6. Data in column D of Table 3 were excluded from further studies because of the incorrect selection of D_{max}, as discussed earlier. It is evident from Table 6 that the effect of D_{min} on the final results varies with the magnitude of D_{min} itself, and with the powder collections under study. For the data in Table 1 and in columns A, B, C of Table 3, D_{min} has little effect on the final results when it is less than *10* μm. As D_{min} increases to *30* μm, distinct effects were observed for all of these data, with the most prominent effect on the data in column B of Table 3. For the data in column E of Table 3, D_{min} has slight effect on the final results when it is *5* μm. As it increases to *10* μm, the effect becomes much more pronounced. When it is set to be *30* μm, the results are completely different from those corresponding to D_{min}=*0*.

Moreover, the standard errors associated with the determined parameters are so huge that the results appear to be of little significance.

Table 6 only demonstrates the possible effect of D_{min} on the final results obtained. In practice, to evaluate the effect of dust separation by cyclone, the true D_{min} corresponding to the cyclone should be evaluated and used in equation (18). Moreover, similar to the removal of coarse powders, if the D_{min} given by the cyclone has extensive effect on the final results such that the results obtained by assuming $D_{min}=0$ is no longer reliable, D_{min} should be adjusted to a lower value by using a different cyclone. This may be very difficult in many situations because of the cost of cyclone. An alternative but also costly method is to employ new techniques, such as *in-situ* characterization techniques.

Table 6. Characteristic parameters and fitting coefficients obtained using equation (18) for data in Tables 1 and 3. D_{max} is the same as that employed in experiment. D_{min} is assumed to be 0, 5, 10 and 30 μm.

parameters		W_t	error	$d_{50}(D_m)$	error	σ	error	fitting
Data	D_{min}	(g)	(%)	(μm)	(%)		(%)	coeff. (%)
table 1	*0, 5,10*	132.0	0.8	74.0	0.8	0.449	2.2	99.971
	30	137.1	1	72.6	0.8	0.475	2.7	99.973
table 3	*0, 5, 10*	1661.1	1.4	86.5	1.8	0.435	5.6	99.754
col. A	*30*	1675.1	1.6	86.0	1.9	0.439	6.3	99.737
table 3	*0, 5, 10*	127.6	0.7	43.7	0.9	0.351	4.8	99.778
col. B	*30*	204.5	15	34.7	9.2	0.456	13	99.617
table 3	*0, 5, 10*	696.5	6.2	61.3	4.8	0.411	14	99.363
col. C	*30*	777.2	12	59.2	4.7	0.477	21	99.412
	0	103.0	1.2	42.3	1.7	0.866	5.1	99.932
table 3	*5*	103.8	1.4	42.0	1.8	0.871	5.2	99.933
col. E	*10*	110.4	2.6	39.5	2.9	0.906	5.9	99.939
	30	1.2×10^5	4000	0.04	4500	2.095	308	98.241

CHAPTER 5. SUMMARY

The procedure conventionally employed to interpret the experimental sieving data was examined. It was demonstrated that the conventional procedure is flawed from several standpoints. Along with several implicit, hard-to-be-justified, assumptions associated with it, the conventional graphical representation procedure also failed to address the reliability of its results. To resolve these problems, a new procedure was formulated. Application of the formulated procedure to several sets of sample sieving data reveals that it is capable of extracting the total weight of powders from experimental data, of determining the nature of size distribution, of characterizing the characteristic parameters, and simultaneously, of determining the reliability of its results.

REFERENCES

1. R. R. Irani and C. F. Callis, *Particle Size: Measurement, Interpretation, and Application*, John Wiley & Sons, New York (1963).
2. T. Allen, *Particle Size Measurement*, Chapman and Hall, London (1981).
3. P. S. Grant, B. Cantor and L. Katgerman, *Acta Metall. Mater.* **41**, 3109 (1993).
4. A. Jeffrey, *Handbook of Mathematical Formulas and Integrals*, Academic Press, San Diego (1995).
5. F. Kottler, *J. Franklin Inst.* **250**, 419 (1950).
6. R. R. Irani, *J. Phys. Chem.* **63**, 1603 (1959).
7. C. Danial and F. S. Wood, *Fitting Equations to Data*, John Wiley & Sons, New York (1980).
8. O. Storch, *Industrial Separators for Gas Cleaning*, Elsevier, Amsterdam (1979).
9. Fisher-Klosterman Inc., Bulletin 218-C, "XQ Series High Performance Cyclones", (1980).
10. R. M. German, *Powder Metallurgy Science*, MPIF, Princeton, N.J. (1984).
11. M. L. Lau, B. Huang, R. J. Perez, S. R. Nutt and E. J. Lavernia, in *Processing and Properties of Nanocrystalline Materials (Proc. Conf.)*, p. 255, Cleveland, OH (1995).
12. R. J. Perez, B.-L. Huang, P. J. Crawford, A. A. Sharif and E. J. Lavernia, *NanoStructured Materials* **7**, 47 (1996).
13. N. Yang, S. E. Guthrie, S. Ho and E. J. Lavernia, *J. Mater. Synth. Proc.* **4**, 15 (1996).
14. R. J. Grandzol and J. A. Tallmadge, *AIChE Journal* **19**, 1149 (1973).

APPENDIX 1. HONORS AND AWARDS

AWARDS RECEIVED

Dates	Award
1996	Silver Medal of the Materials Science Division of ASM International
1995	Best Paper Award, with X. Liang and J. Wolfenstine, Journal of Thermal Spray Technology
1995	Alexander Von Humboldt Fellowship from Germany
1993	Fellowship from the Iketani Science and Technology Foundation, Tokyo, Japan
1993	ASM International 1993 Bradley Stoughton Award for Young Teachers
1993	Elected to Who's Who in Science and Engineering
1992	Elected to National Honorary Society of Alpha Kappa chapter of Phi Delta Beta
1992	Elected to 2000 Notable American Men
1991	Elected to American Men and Women of Science
1991	Elected to Who's Who in the West
1990-1993	Young Investigator Award, Office of Naval Research (ONR)
1990-1992	Aluminum Company of America (ALCOA) Fellowship
1989-1994	Presidential Young Investigator, National Science Foundation (NSF)
1989-1990	Outstanding Assistant Professor, School of Engineering, UCI
1989	Faculty Career Development Award, University of California, Irvine
1982-1984	Rockwell International Fellowship
1982	George H. Main 1945 Fund Award, Brown University
1978	Alfred J. Loepsinger Scholarship, Brown University

MEMBERSHIPS IN BOARDS OF REVIEW
AND ADVISORY ROLES

Dates	Description
1998	Editor *Material Science and Engineering A*
1996	Advisory Board *Key Engineering Materials*, Trans. Tech
1996	Board of Review *International Journal of Non-Equilibrium Processing*
1996 May 21-24	Member of NSF's Panel on Materials Research Science and Engineering Centers
1996 April 15-17	Member of NSF's Panel on Materials Research Science and Engineering Centers
1996	Co-Editor *Journal of Materials Synthesis and Processing*
1996	ASM International Chair of*Bradley Stoughton Award Committee*
1995	Member of NASA's Headquarters Review Panel on Microgravity in Materials Science
1994-1996	ASM International *Bradley Stoughton Award Committee*
1994	Advisory Board, *Advanced Composites Newsletter*
1994	Board of Review *Journal of Applied Composite Materials*
1994	Board of Review *Metallurgical and Materials Transactions*
1993, 1994	National Research Council's Review Board on NSF Graduate Fellowships Program
1993	Advisor for the Composites Committee *Journal of Metals*
1993	Invited Scientist, technical exchange, The Korea-U.S. *Joint Symposium on Advanced Materials*
1992	National Science Foundation's *Manufacturing Initiative*

APPENDIX 2. PERSONNEL

SENIOR RESEARCH PERSONNEL:

E.J. Lavernia, Professor

GRADUATE STUDENTS:

B. Li, Ph. D Candidate

STAFF:

I. Sauer, Research Technician